Influence of the Defects in a Graphene Oxide on the Reduction via Ascorbic Acid for Structuring Aerogels

Camila Miranda Fonseca Duarte[1,2*], Eliel Gomes da Silva Neto[3], Iara de Fatima Gimenez[2]
[1]SENAI CIMATEC University; Salvador, Bahia; [2]Federal University of Sergipe; Aracaju, Sergipe; [3]Federal University of Bahia; Salvador, Bahia, Brazil

Studies of graphene oxide (GO) have reached new structural possibilities by controlled reducing reactions using ascorbic acid. With the ability of selective reduction, this acid induces the tailoring effect of the sheets, causing a porous lattice. The present study proposes an investigation onto the quality of graphene oxide produced using Hummers' method to understand the reduction mechanism of ascorbic acid better. X-ray diffractometry, Fourier transform infrared spectroscopy with attenuated total reflectance and Raman Spectroscopy analyses were performed. The sample presented a typical crystalline structure of GOs, with appreciable degrees of oxidation and moderate density of defects—promising characteristics in forming the porous network of aerogels.
Keywords: Graphene Oxide. Hummers' Method. Ascorbic Acid. Graphene Oxide Reduction. Lattice Defects.

The need for more practical alternatives to obtain graphene allowed the discovery of derivatives with notable applicability, such as graphene oxide (GO). This material, the oxidized, non-stoichiometric version of graphene, is commonly produced by the chemical exfoliation reaction of graphite [1]. In this reaction, oxygenated functions (hydroxyls, epoxy, carboxyls, and carbonyls) react with the graphene sheets, expanding the lamellae of the graphite structure. Subsequently, effective exfoliation takes place through sonication in suspension, yielding sheets of different sizes, stacking (mono, bi, and a few layers), and degrees of oxidation [2,3]. This material can also be reduced, removing these oxygenated functions from its sheets, achieving appreciable purities, and restoring the properties of graphene.

Hydrazine has established itself as the most effective reducing agent among the reduction alternatives. However, the toxicity of its reaction products and environmental damage have demanded new, safer, and more eco-friendly alternatives [4,5]. Thus, ascorbic acid emerges as a suitable alternative to meet both requirements, ensuring high efficiency in reducing the oxidized sheets with practically non-toxic by-products. As an additional benefit, it also produces reduced graphene with a larger specific surface area, compared to hydrazine, by acting indirectly as a separator between the sheets, forming a porous network and producing hydrogels [6,7].

Nevertheless, reduction and oxidation are critical processes for the structure of the resulting graphene sheets. Both excess oxidation and oxidative precursors can cause defects in the graphene network that directly affect the subsequent reduction activity. This occurs since, under more aggressive oxidations, the continuity of the graphene network is affected, increasing the number of defects, which, for the most part, are considered edge zones [8,9].

In the case of ascorbic acid, its primary reduction target is the oxygenated functional groups in the basal plane (hydroxyls and epoxy groups). At the same time, the edge species (carboxyls and carbonyls) are less influenced. Additionally, edge species will interact with each other through hydrogen bonds [7,8], causing a tailoring effect between the sheets and promoting a hierarchical porosity structure [6].

The possibility of obtaining these porous structures, known as graphene aerogels, from a simple methodology based on the environmentally friendly reduction of GO draws attention due to

Received on 18 September 2024; revised 28 November 2024.
Address for correspondence: Camila Miranda Fonseca Duarte.Rua Luís Eduardo Magalhães, 192, itapuã. Zipcode: 41630-700. Salvador, Bahia, Brazil. E-mail: camila.duarte@fieb.org.br.

J Bioeng. Tech. Health 2024;7(4):342-347

the numerous possible applications. However, understanding the structure of the graphene oxide precursor and how it will influence the reduction mechanism of ascorbic acid is essential to achieving stable aerogel structures [10]. Therefore, the present work sought to evaluate the quality of graphene oxide produced by the Hummers method, relating its defects and network to the reducing action of ascorbic acid to form aerogels.

Materials and Methods

The method adopted for synthesizing graphene oxide was based on the work of Yoo M and Park H [11], which uses the Hummers method. Initially, 5 g of graphite was added to a beaker containing 115 mL of H_2SO_4 in an ice bath (approx. 6 °C) and stirred for one hour. Then, 15 g of $KMnO_4$ was slowly added to the system, controlling the temperature, kept under stirring at 40 °C for 3 hours. Finally, 230 mL of distilled water was carefully added to the system to dilute it, avoiding the sudden rise of the temperature so as not to exceed 90 °C, for 30 min under continuous stirring, then further 115 mL of H_2O_{dest} to cool the solution to room temperature. Upon reaching 35 °C, 15 mL of H_2O_2 was added to the system under continuous stirring for another 15 min to stop the reaction.

Finally, the stirring stopped, and the solution was allowed to settle overnight. The supernatant was removed, and the decanted cake was washed in 500 mL HCl 10%, under agitation for 1 h, and then allowed to settle.This process was repeated twice, and the decanted product was vacuum filtered in a Buchner funnel with a glass fiber filter. The cake obtained was dried under mild conditions (40 °C) overnight, resulting in a monolith, which was stored in a container isolated from light and named GO.

The material obtained was subjected to X-ray diffractometry (XRD) performed on a Shimadzu XDR-6000 diffractometer, with CuKα radiation, 40 kV, 30 mA, graphite monochromator, in a scanning range of 5° to 80° with a step of 2 °/min. The RAMAN spectrum was obtained using a JASCO 5200 instrument with a laser width of 532 nm and 0.3 mW of power. The Fourier transform infrared spectroscopy with Attenuated Total Reflectance (FTIR-ATR) was performed using a Thermo Scientific Nicolet iS10 spectrometer at room temperature in the 500-4000 cm^{-1} range. Micrographs were also obtained using a Jeol JEM1400 plus Transmission Electron Microscope (TEM) operating under a voltage of 120 kV.

Results and Discussion

The diffractogram obtained in the GO sample (Figure 1) presents two prominent peaks at 10.38° and 42.32°, characteristic of the graphene oxide structure, according to the literature [4,12,13]. It is well known that the central peak of graphite occurs at $2\theta \approx 26.4°$, referring to the {002} plane, having an interplanar distance of 3.375 Å [12]. After being subjected to the oxidative process, the graphite lamellae are expanded by the intercalated oxygenated species, causing an increase in the d- d-spacing of the structure. This effect features by the appearance of the peak at 10.38°, which, by Bragg's Law, reflects an interplanar distance of ~ 8.5 Å and denotes the interlayer expansion of the {001} plane, confirming the efficiency of the oxidative process in the intercalation of graphite [14,15]. The second peak, located at $2\theta = 42.32°$, refers to the {101} plane of the sp^2 graphitic lattice, present mainly in graphene oxides whose precursor is synthetic graphite [12], as this present methodology. It is worth mentioning that the width of the observed peaks is due to the high distribution of the sheet sizes, which can be interpreted as a reflection of the randomness of the crystallite sizes, also characteristic of the GO samples.

When analyzing the spectra obtained by FTIR-ATR (Figure 2), it is possible to notice an abundance of oxygenated functions present in the GO sample; for instance, -OH, C=O, and C-O-C, reinforcing the hypothesis that the oxidation of the graphite sheets was effective, in agreement with the peak shift seen in the XRD results. The broad zone between

Figure 1. A diffractogram of the sample was obtained using Hummers' method.

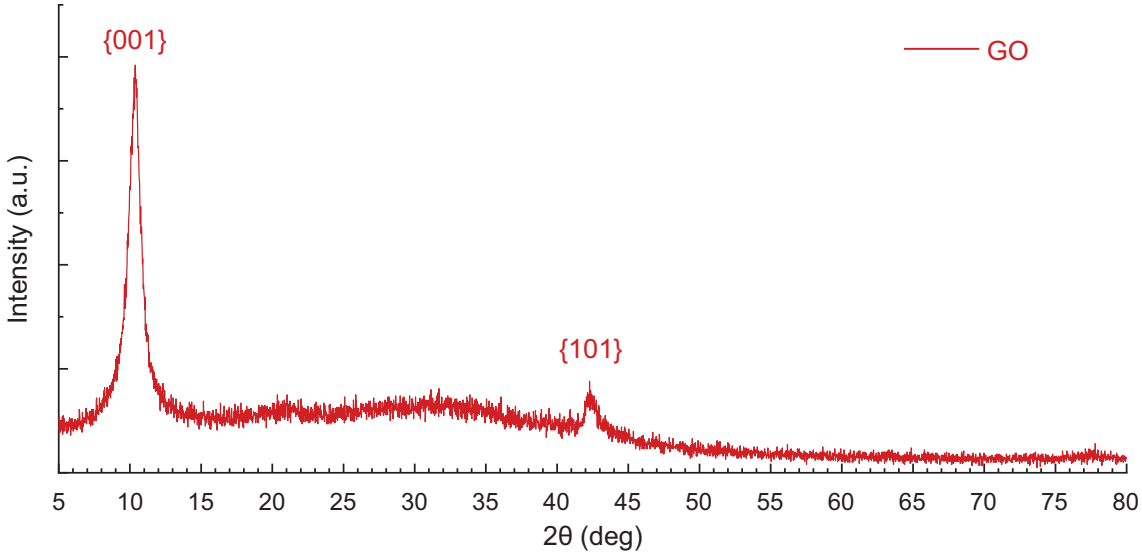

Figure 2. FTIR-ATR spectrum of graphene oxide sample obtained via Hummers.

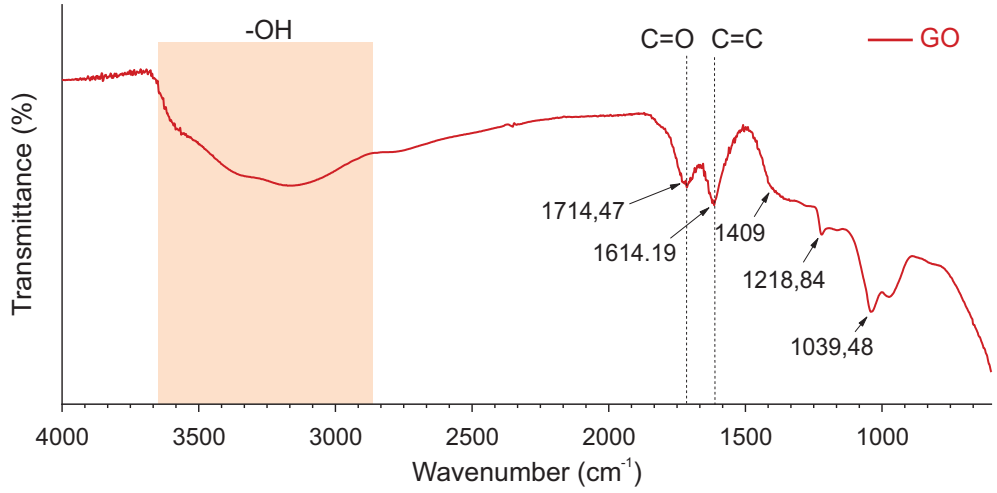

3600 and 2900 cm^{-1}, highlighted in red in Figure 2, frequently seen in graphene oxides, refers to the presence of hydroxyl groups, usually linked to the network in the basal plane [3,16] or even associated with carboxylic groups. In addition, the two leading characteristic bands of GO were also identified, in 1714 and 1614 cm^{-1}, consistent with those found in the literature [7,16], endorsing the understanding that the sample is a graphene oxide, attesting to the effectiveness of the synthesis. Carboxylic acid (shoulder ~1400 cm^{-1}) and epoxy (1218.84 and 1039.48 cm^{-1}) structures were also identified in the spectrum [13].

When observing the Raman spectrum of the GO sample obtained (Figure 3), the presence of two peaks, characteristic of graphene oxide [17,18], centered at 1346 and 1601 cm^{-1}, referring to the D and G bands, respectively, is noted. The D band reflects the degree of disorder linked to the defects present in the lattice. This band does not appear in perfect graphene and is, therefore, related to a mechanism where the presence of defects activates

phonons outside the center of the Brillouin zone in a double resonance process; the G band, on the other hand, refers to the vibration of the sp^2 bonds of the basal plane, being usually observed in perfect graphene spectra. However, changes in its position and width can be associated with the sheets' oxidation level. In the presence of defects, a band called D' near the G band region is responsible for some of the broadening and displacement effects (Figure 4) [17–19]. In the high-energy region of the spectrum, above 2500 cm^{-1}, second-order 2D, D+D', and 2D' bands of low intensity were identified, which is expected in graphene.

Figure 3. RAMAN spectrum of graphene oxide sample produced by Hummers.

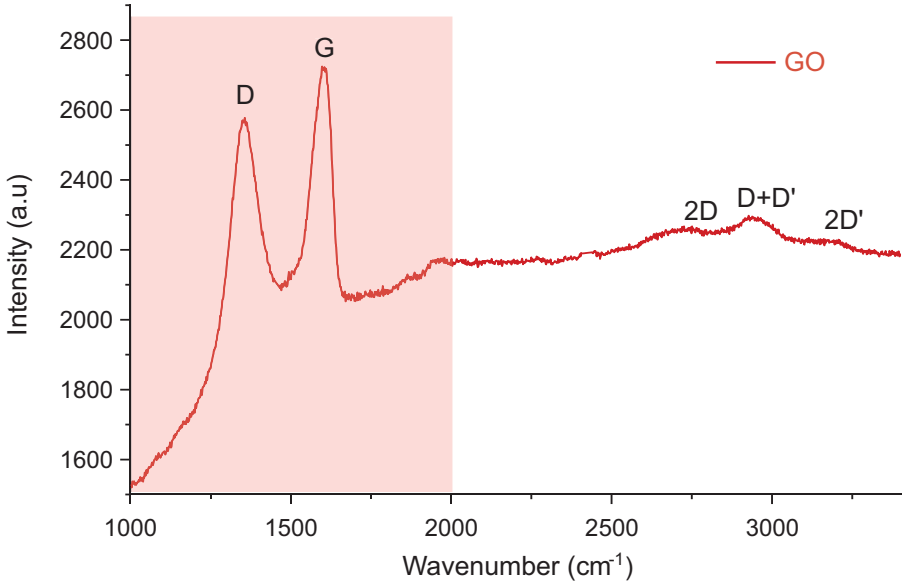

Figure 4. Deconvolution of the RAMAN spectrum in the D and G band region (on left) and micrographs obtained via TEM of the sample after exfoliation (on right).

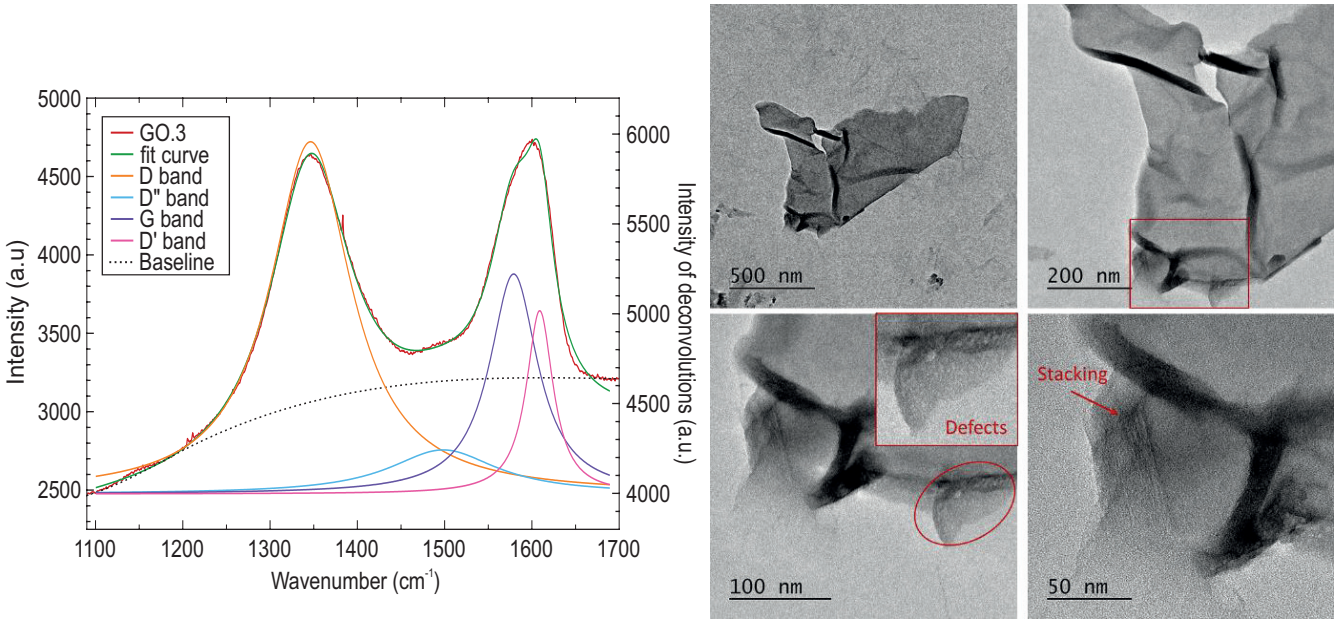

Derivatives with a certain degree of defects, such as the synthesized sample, occur because the relationship between the intensities of the 2D and DD+D bands reflects the C sp² density of the GO sheets [18].

To better understand the structure of the synthesized GO and evaluate the quality of its sheets, the deconvolution of the Raman spectrum was performed using Lorentzian functions (Figure 4) [19]. The presence of the D'', D, G, and D' bands was identified, with their peaks located at 1498.37 cm^{-1}, 1346.40 cm^{-1}, 1579.11 cm^{-1}, and 1608.97 cm^{-1}, respectively.

From the curve fit data, the degree of disorder of the sample was calculated using the ratio of the area under the curve of the D and G bands (AD/AG) since they represent the probability of phonon scattering. In the sample, this ratio is 2.69, which characterizes the synthesized graphene oxide with a low to moderate degree of disorder [18,19]. Furthermore, according to Lopez-Díaz D. and colleagues [18], in values of AD/AG 3.5, it is possible to identify the type of defect with the highest incidence in the material by evaluating the ratio AD'/AD, which in the analyzed sample presented a value of 0.17, indicating the coexistence of vacancy defects (0.14) and crystallite edges (0.29), with a predominance of vacancies [18]. The presence of the D' and D'' bands, with noticeable intensities, further supports the understanding of the significant presence of defects since the first indicates the presence of impurities in the graphene network, which can be associated with the oxygenated functions present in the sheets. The second reflects the degree of amorphicity of the sample, which in turn is also influenced by the small crystallite sizes [18,19]. TEM images in Figure 4 (on the right) show a structure of the GO sample after exfoliation, where smooth edge zones can be noted, characteristic of armchair configurations [20], in addition to perforations in the sheets resulting from the oxidative process and zones indicative of sheet stacking. Using Raman spectroscopy, we can also estimate the average crystallite size through Equation 1 [13]

Equation 1.

$$L_a = \frac{2{,}4E^{-10}\ x\ (\lambda_{laser})^4}{(A_D/A_G)}$$

Considering the laser wavelength (λ_{laser}) of 532 nm and applying the values from the curves, an average crystallite size of 7.1 nm was found. This size can be interpreted as the distance between the defects in the graphene sheet; the smaller this size, the greater the density of defects in our sample [17,18].

The characteristics obtained were evaluated according to the ascorbic acid reduction mechanism, aiming to preliminarily predict how the material will behave to form the porous network of the reduced graphene oxide aerogel. Therefore, when analyzing the average crystallite size with the identified oxygenated species, the synthesized GO presents a high edge zone where -COOH and C=O species are predominant. On the other hand, the literature indicates that the reducing action of ascorbic acid is concurrent with the formation of the porous network and has selectivity for the epoxy and -OH groups located in the basal plane, while those at the edges are less influenced, enabling an interaction of the sheets by hydrogen bonds, which induces the formation of hydrogel agglomerates [6–8].

Still, another critical point to be observed in structuring a stable porous network is the overlapping of the sheets forming the walls. In the reduction process via ascorbic acid, the parallel stacking of the sheets is influenced by their size. This is because the presence of the edge functions causes steric effects, generating a random interaction between the edges and basal planes of the sheets smaller than 10 nm, while in dimensions greater than 80 nm, the basal functions prevent the effective stacking connection between layers, which can result in low structural stability of the aerogel [10]. Still, other synthesis parameters also directly interfere with quality, such as pH, agitation, and temperature reduction, and must be considered to obtain structures per the desired objective.

Conclusion

It is concluded that the GO obtained has a moderate defect degree, most of which are vacancies, as indicated in the FTIR. Raman spectroscopy measurements revealed that the average crystallite diameter was approximately 7.1 nm. The small size represents a reasonable but not very intense defect density, which is interesting since starting from an exfoliated and less damaged GO is an advantage, which means that the oxygenated edge species will also be predominant in the sample, as identified by the bands corresponding to the -COOH and C=O structures in the FTIR-ATR spectrum. These characteristics are promising for forming a porous network in this material, which is spontaneous and structured since the starting GO has sufficient edge functions for the tailoring effect of the sheets, which are responsible for generating the aerogel structure. Other parameters such as sheet size, degree of reduction, and ordered stacking are effects of complementary synthesis methods that are being studied by the team for future work.

Acknowledgments

The authors thank the institutions SENAI CIMATEC and Federal University of Bahia for their contribution to the infrastructure needed to carry out the experiments and characterizations presented in this work.

References

1. Coros M, Pogăcean F, Măgeruşan L et al. A brief overview on synthesis and applications of graphene and graphene-based nanomaterials. Front Mater Sci 2019:23–32.
2. Chen X, Qu Z, Liu Z et al. Mechanism of oxidization of graphite to graphene oxide by the Hummers method. ACS Omega 2022;7:23503–23510.
3. Hou Y, Lv S, Liu L et al. High-quality preparation of graphene oxide via the Hummers' method: Understanding the roles of the intercalator, oxidant, and graphite particle size. Ceram Int 2020;46:2392–2402.
4. Bychko I, Abakumov A, Didenko O et al. Differences in the structure and functionalities of graphene oxide and reduced graphene oxide obtained from graphite with various degrees of graphitization. Journal of Physics and Chemistry of Solids 2022;164.
5. Stobinski L, Lesiak B, Malolepszy A et al. Graphene oxide and reduced graphene oxide studied by the XRD, TEM and electron spectroscopy methods. J Electron Spectros Relat Phenomena 2014;195:145–154.
6. Ortiz-Anaya I, Nishina Y. Unveiling the reduction process of graphene oxide by ascorbic acid: Grafting and reduction sequences for high surface area graphene materials. Chempluschem 2023;88.
7. Palomba M, Carotenuto G, Longo A. A brief review: The Use of L-ascorbic acid as a green reducing agent of graphene oxide. Materials 2022;15.
8. de Silva KKH, Huang HH, Yoshimura M. Progress of reduction of graphene oxide by ascorbic acid. Appl Surf Sci 2018;447:338–346.
9. Li M, Deng T, Zheng B et al. Effect of defects on the mechanical and thermal properties of graphene. Nanomaterials 2019;9.
10. Lee SP, Ali GAM, Hegazy HH et al. Optimizing reduced graphene oxide aerogel for a supercapacitor. Energy and Fuels 2021;35:4559–4569.
11. Yoo MJ, Park HB. Effect of hydrogen peroxide on properties of graphene oxide in Hummers method. Carbon N Y 2019;141:515–522.
12. Kim JH, Shim GH, Vo TTN et al. Building with graphene oxide: effect of graphite nature and oxidation methods on the graphene assembly. RSC Adv 2021;11:3645–3654.
13. Hou Y, Lv S, Liu L et al. High-quality preparation of graphene oxide via the Hummers' method: Understanding the roles of the intercalator, oxidant, and graphite particle size. Ceram Int 2020;46:2392–2402.
14. Iakunkov A, Talyzin A V. Swelling properties of graphite oxides and graphene oxide multilayered materials. Nanoscale 2020;12:21060–21093.
15. Yu W, Sisi L, Haiyan Y et al. Progress in the functional modification of graphene/graphene oxide: A review. RSC Adv. Royal Society of Chemistry 2020;15328–15345.
16. Hiosseini MA, Malekie S, Ebrahimi N. The analysis of linear dose-responses in gamma-irradiated graphene oxide: Can FTIR analysis be considered a novel approach to examining the linear dose-responses in carbon nanostructures? Radiation Physics and Chemistry 2020;176.
17. Anusuya T, Pathak DK, Kumar R et al. Deconvolution and quantification of defect types from the first order Raman spectra of graphene oxide derivatives. FlatChem 2022;35.
18. López-Díaz D, Delgado-Notario JA, Clericò V et al. Towards understanding the Raman spectrum of graphene oxide: The effect of the chemical composition. Coatings 2020;10.
19. Lee AY, Yang K, Anh ND et al. Raman study of D' band in graphene oxide and its correlation with reduction. Appl Surf Sci 2021;536.
20. Lee XJ et al. Review on graphene and its derivatives: Synthesis methods and potential industrial implementation. J Taiwan Inst Chem Eng 2019;98:163–180.